JTAM (Jurnal Teori dan Aplikasi Matematika)
http://journal.ummat.ac.id/index.php/jtam
p-ISSN 2597-7512 | e-ISSN 2614-1175
Vol. 9, No. 3, July 2025, pp. 1040-1052

Modeling Spatio-Temporal Precipitation Patterns in East Kalimantan using Space-Time Kriging and Median Polish-Based Spatio-Temporal Kriging

Friendtika Miftaqul Jannah[1*], Rahma Fitriani[1], Henny Pramoedyo[1]
[1]Department of Statistics, Brawijaya University, Indonesia
friendtika@student.ub.ac.id

Article History:
Received : 18-04-2025
Revised : 19-05-2025
Accepted : 28-05-2025
Online : 05-07-2025

Keywords:
Kriging;
Precipitation Modeling;
Prediction Accuracy;
Spatio-Temporal.

ABSTRACT

Precipitation variability presents significant challenges for disaster risk reduction and water resource management, particularly in flood and drought-prone regions such as East Kalimantan. This study aims to develop and evaluate two statistical approaches for spatio-temporal precipitation modeling: spatio-temporal kriging (ST-Kriging) and spatio-temporal median polish kriging (ST-MPK). Using monthly precipitation data obtained from seven observation stations provided by BMKG and BPS for the period 2021 to 2023, both models were assessed using performance metrics. ST-Kriging employed a simple sum-metric semivariogram model that combines exponential spatial and Gaussian temporal components. This model achieved an RMSE of 84.05, MAE of 69.95, and MAPE of 52.67%. Meanwhile, ST-MPK model, incorporating robust median polish decomposition and ST-Kriging of residuals, produced a lower MAPE of 44.83% with higher RMSE (122.44) and MAE (91.35). This suggests that while ST-Kriging offers better absolute error performance, ST-MPK provides greater relative accuracy and improved robustness to outliers, critical advantages for modeling precipitation in regions undergoing environmental shifts, where anomalies and extremes are increasingly common. These findings highlight ST-MPK's potential to produce more reliable forecasts under irregular precipitation conditions, supporting early warning systems and informed water resource planning. Scientifically, this research contributes a robust modeling framework suitable for data-scarce and outlier-prone contexts. Practically, it can aid policymakers in designing adaptive flood mitigation strategies and sustainable water management policies tailored to the evolving climate realities of East Kalimantan.

https://doi.org/10.31764/jtam.v9i3.30642

A. INTRODUCTION

East Kalimantan has undergone a major transformation following its designation as the relocation site for Indonesia's new National Capital (IKN). This transition has triggered large-scale land use and land cover (LULC) changes, such as deforestation and urban expansion, which can directly impact regional precipitation patterns (Yang et al., 2020). Specifically, the replacement of forested areas with impervious surfaces (e.g., asphalt and concrete) alters the surface energy balance, disrupts evapotranspiration processes, and modifies local convection patterns factors known to influence cloud formation and precipitation distribution (Sari & Atsidiqi, 2020; Sudinda, 2020). As a result, hydrological cycles in the region may become more variable, increasing the frequency and intensity of extreme weather events, including localized heavy precipitation and flooding (Adiguna et al., 2021; Pertiwi et al., 2015).

Understanding how these environmental changes affect precipitation dynamics is essential for supporting sustainable development in IKN. Accurate spatio-temporal modeling of precipitation is a critical component of flood risk management, infrastructure planning, and the long-term sustainability of water resources. It enables the identification of high-risk zones and supports proactive interventions such as green infrastructure and land restoration (Chen et al., 2021; Olanrewaju et al., 2017; Zhang et al., 2020). Precipitation patterns often demonstrate strong spatial and temporal heterogeneity due to atmospheric events, local geography, and microclimates, which complicates prediction and modeling (Katipoğlu, 2022; Varouchakis et al., 2021; Zhang et al., 2020). Therefore, advanced geostatistical and time-series modeling techniques are required to ensure high prediction accuracy in both observed and unobserved areas.

To address this, advanced modeling techniques are required. Spatio-temporal kriging (ST-Kriging) is widely recognized in hydrology for its capacity to produce smooth and continuous precipitation surfaces over space and time, especially when observational data are sparse. It leverages the semivariogram to model spatial autocorrelation and incorporates temporal variation, offering a statistically rigorous approach to estimating unmeasured values (Abdullah et al., 2018; Liu & Tung, 2020; Verdin et al., 2016). The method has evolved into ST-Kriging, which integrates spatial and temporal dimensions to improve prediction accuracy in datasets with dynamic changes over time and space (Varouchakis et al., 2021). Its use is particularly relevant in East Kalimantan where rapid urban development introduces high spatial variability in precipitation that must be captured accurately for decision-making. Prior investigations have confirmed the method's ability to deliver precise and reliable interpolation outcomes. For instance, Raja et al. (2017) demonstrated that ST-Kriging effectively characterizes precipitation variability patterns, generating smoother and more consistent predictions than methods limited to spatial interpolation alone. Furthermore, the technique facilitates the detection of anomalies and long-term precipitation trends, which are vital components in managing water resources and preparing for natural disasters. Complementary findings by De Carvalho et al. (2016) also emphasized that ST-Kriging offers more accurate daily precipitation estimates, as indicated by reduced mean square error and improved correlation between observed and predicted values when compared to traditional kriging and cokriging methods. These advantages underscore the potential of ST-Kriging in analyzing precipitation dynamics across space and time, thereby supporting more precise planning for flood prevention and sustainable water management.

Nevertheless, a key limitation of ST-Kriging is its sensitivity to extreme values (outliers), both of which are common in tropical precipitation datasets due to intense and erratic precipitation events (O'Leary et al., 2016). In response to these limitations, Jannah et al. (2025) proposed the Spatio-Temporal Median Polish Kriging (ST-MPK), which combines robust median polish decomposition for trend extraction, kriging for spatial interpolation, and ARIMA for temporal modeling. This method enhances robustness by using median-based estimators, which are less influenced by outliers, and is particularly suited to precipitation modeling in regions experiencing frequent hydrometeorological extremes (X. L. Sun et al., 2019). Despite its innovation, the ST-MPK method has not been empirically validated against ST-Kriging using real-world precipitation data. Jannah et al. (2025) focused on methodological development without conducting a model performance comparison, leaving a critical gap in the literature. Consequently, it remains unclear whether ST-MPK provides superior predictive accuracy or robustness in practical applications, particularly in transitional urban-environmental contexts like East Kalimantan.

To fill this research gap, the present study aims to construct and compare the accuracy of two precipitation modeling techniques: ST-Kriging and ST-MPK, using the same dataset of monthly precipitation observations in East Kalimantan from 2021 to 2023. This comparative evaluation is designed to provide empirical evidence on which method yields better prediction performance across multiple statistical metrics. Given the region's evolving climatic and land-use dynamics, selecting an optimal modeling approach is crucial for generating reliable precipitation forecasts, which are essential for effective flood mitigation planning and sustainable water resource management in East Kalimantan.

B. METHODS

This study is a quantitative study employing a spatio-temporal modeling approach to analyze precipitation patterns in East Kalimantan. The study compares the predictive performance of two models: spatio-temporal kriging (ST-Kriging) and spatio-temporal median polish kriging (ST-MPK). All statistical analyses were conducted using R software.

1. Data Description

The study utilizes secondary monthly precipitation data from the Meteorological, Climatological, and Geophysical Agency (BMKG) of Samarinda. The dataset includes:

a. Total monthly precipitation (mm),
b. Geographic coordinates (latitude and longitude),
c. Time span: January 2021 to December 2023,
d. Seven observation stations located in Samarinda, Balikpapan, Berau, East Kutai, Kutai Kartanegara, West Kutai, and Bontang.

2. Stationarity Testing

Spatio-temporal stationarity implies that data variation is influenced only by spatial and temporal lags, not by specific locations or time points. Stationarity testing purpose to detect whether precipitation values vary systematically by location and to determine the existence of a unit root and decide whether differencing is required. One common approach to evaluating spatio-temporal non-stationarity is through semivariogram analysis, which facilitates the identification of spatial and temporal trends or irregularities in the dataset (Shand & Li, 2017).

a. Stationarity in spatial data

   Spatial non-stationarity occurs when observations vary with geographic coordinates. This can be identified by plotting data against longitude and latitude for each time step (Rohma et al., 2023), and confirmed using regression analysis. If trends are detected, a Box-Cox transformation is recommended, particularly when $\lambda \neq 1$ or lies outside the 95% confidence interval.

b. Stationarity in temporal data

To test temporal stationarity, especially in panel data, the Im-Pesaran-Shin (IPS) unit root test is applied. This method uses the average of Dickey-Fuller statistics across panels (Murthy & Okunade, 2018). Differencing ($\Delta Z_t = Z_t - Z_{t-1}$) is used if non-stationarity is present.

3. Spatio-Temporal Semivariogram Modeling

The semivariogram characterizes the degree of spatial and temporal autocorrelation as a function of lag distance and time difference, which is essential for determining weights in kriging interpolation.

a. Empirical Semivariogram

The empirical semivariogram is estimated using the method of moments, which computes the average squared difference between paired observations within defined spatial and temporal lag tolerances (Yang et al., 2020).

b. Theoretical Semivariogram Models

To facilitate kriging, theoretical semivariogram functions were fitted to the empirical semivariograms. The exponential and gaussian models were employed independently for spatial and temporal components. In the spatial component, which uses distance h, the equation model is as follows.

1) Exponential model

$$\gamma(|\boldsymbol{h}|) = c_0 + c\left\{1 - exp\left(-\frac{|\boldsymbol{h}|}{a}\right)\right\} \tag{1}$$

2) Gaussian model

$$\gamma(|\boldsymbol{h}|) = c_0 + c\left\{1 - exp\left(-\frac{|\boldsymbol{h}|^2}{a^2}\right)\right\} \tag{2}$$

where:

$\gamma(|\boldsymbol{h}|)$: semivariance at lag or distance h

c : a priori variability of the autocorrelation process

c_0 : nugget, a spatially uncorrelated semivariance representation at distances smaller than the measurement error and sampling interval

a : *range*, the distance over which spatial autocorrelation or dependence persists. There is a correlation between values at distance closer than a, but no correlation between those at greater distance

$c_0 + c$: *sill*, representing the point where the large diversity reaches a constant value

The same equation model is applied to the temporal component using the temporal distance or lag u. For joint spatio-temporal structures, several models are used:

1) Metric model

Account for space-time interactions by combining spatial and temporal lags into a single metric whose semivariogram function is shown in equation (3).

$$\gamma(\boldsymbol{h},u) = \gamma\sqrt{\|\boldsymbol{h}\|^2 + (k.|u|)^2},\ \ (\boldsymbol{h},u) \in \mathbb{R}^d \times \mathbb{R}, c > 0 \tag{3}$$

where $\|\boldsymbol{h}\| + c|u|$ is the distance on $\mathbb{R}^d \times \mathbb{R}$ and c is a positive contant.

2) Sum-metric model
In semivarogram terms, the combined metric-sum model is given by equation (4).

$$\gamma(\boldsymbol{h},u) = \gamma_s(\boldsymbol{h}) + \gamma_t(u) + \gamma\sqrt{\|\boldsymbol{h}\|^2 + (k.|u|)^2}, (\boldsymbol{h},u) \in \mathbb{R}^d \times \mathbb{R}, c > 0 \tag{4}$$

3) Simple sum-metric model
Includes a nugget effect and adds spatial, temporal, and joint lag terms with the semivariogram function shown in equation (5).

$$\gamma(\boldsymbol{h},u) = c_0 + \gamma_s(\boldsymbol{h}) + \gamma_t(u) + \gamma\sqrt{\|\boldsymbol{h}\|^2 + (k.|u|)^2}, (\boldsymbol{h},u) \in \mathbb{R}^d \times \mathbb{R}, c > 0 \tag{5}$$

4. Spatio-Temporal Kriging

ST-Kriging is employed to estimate the unknown value $Z(s_0, t_0)$ at a location and time where data are not observed (s_0, t_0). This prediction uses available observations from across the region or within selected neighborhoods. The process is based on a spatio-temporal random field $\{Z(\boldsymbol{s},t), \boldsymbol{s} \in D, t \in T\}$, with $D \subseteq \mathbb{R}^2$ and $T \subseteq \mathbb{R}$, and assumes that values have been recorded at n spatio-temporal locations $\{Z(s_1,t_1), \dots, Z(s_n,t_n)\}$. The predicted value is calculated as a weighted sum of observations (Montero et al., 2015).

$$\hat{Z}(\boldsymbol{s}_0, t_0) = \sum_{i=1}^{n} \lambda_i Z(\boldsymbol{s}_i, t_i) \tag{6}$$

where $\hat{Z}(\boldsymbol{s}_0, t_0)$ is the value at a location and time that is not observed, $Z(\boldsymbol{s}_i, t_i)$ are the value at an observed location and time, and λ_i are the weights derived under the assumption of second-order stationarity. The weights are obtained by solving a system based on the semivariogram between observed points and between observed and target locations.

5. Spatio-Temporal Median Polish Kriging Modeling

ST-MPK enhances robustness in modeling by decomposing the precipitation data matrix into additive components representing spatial, temporal, and residual effects. This decomposition helps isolate systematic trends and reduce the influence of outliers commonly found in precipitation data.

a. Median Polish Decomposition
Median polish is employed due to its robustness against outliers and its nonparametric nature, making it well-suited for environmental data that often exhibit non-normal distributions and extreme values. By using medians rather than means, the method minimizes the impact of anomalous observations while effectively separating systematic variations attributable to spatial and temporal effects. This separation allows for better

modeling of localized deviations and interaction effects through the residuals. The two-way median polish model is used to separate spatial and temporal effects, which can be showed as equation (7).

$$Z(\boldsymbol{s}, t) = \mu + \alpha_l + \tau_t + e \tag{7}$$

μ represents the general effect, α_l is the l-th row effect representing the spatial effect, dan τ_t is the t-th column effect representing the time effect, e is the error term. The effects α_l (spatial) and τ_t (temporal) are obtained through iterative procedures and residual medians (Martínez et al., 2017).

b. Median Polish Spatial Effects Modeling with Kriging
Kriging is used to model the spatial effects α_l with weights λ_i calculated based on a semivariogram. Theoretical semivariogram models such as exponential and Gaussian are applied according to the characteristics of the precipitation data.

c. Median Polish Time Effects Modeling with ARIMA
The temporal effects τ_t are modeled using $ARIMA(p, d, q)(P, D, Q)_S$, through the stages of stationarity checking, model identification, parameter estimation, and diagnostic testing. Forecasting is performed for future values based on the best-selected model.

d. Median Polish Residuals Modeling with Spatio-Temporal Kriging
The residuals from the median polish model are modeled using ST-Kriging. Various spatio-temporal semivariogram models are considered, including the product-sum, metric, and sum-metric models.

e. Spatio-Temporal Median Polish Kriging
The final model combines all components:

$$\hat{Z}(\boldsymbol{s_0}, t_0) = \hat{\mu} + \sum_{i=1}^{n} \lambda_i \alpha(\boldsymbol{s}_i) + \hat{\tau}_t + \sum_{i=1}^{n} \lambda_i e(s_i, t_i) \tag{8}$$

with $\hat{\mu}$ is general mean, λ_i are weights, $\alpha(\boldsymbol{s}_i)$ are the data at an observed locations and times, $\hat{\tau}_t = \frac{\hat{\theta}_0 + \hat{\theta}_q(B)\hat{\Theta}_Q(B^S)a_t}{\hat{\Phi}_P(B^S)\hat{\phi}_p(B)(1-B)^d(1-B)^D}$, $e(s_i, t_i)$ are the residuals from the median polish model. This model enables prediction at unobserved locations and times by integrating the spatio-temporal structure of the median polish, kriging, and ARIMA methods.

6. Model Performance

The model is evaluated using RMSE (Root Mean Square Error), MAE (Mean Absolute Errors), and MAPE (Mean Absolute Percentage Error) (Islam et al., 2024; Ruslana et al., 2024).

C. RESULT AND DISCUSSION

1. Stationary Data

Descriptive analysis shows that precipitation in East Kalimantan is spatially stationary, as indicated by the random distribution across coordinates and the empirical semivariogram (Figure 1 & Figure 3), which shows no spatial trend. Regression tests on easting and northing yield $p - values\ > 0.05$, indicating no significant spatial effect. Temporally, the data is also stationary, supported by the average Dickey-Fuller statistic of -4.80 and IPS test statistic of -9.742 with a p-value of $1{,}0 \times 10^{-6}$, thus rejecting the null hypothesis of non-stationarity. Since the mean precipitation is unknown, the spatio-temporal ordinary kriging model is appropriate. Long Iram station recorded the highest precipitation, likely due to orographic effects and local vegetation (Figure 2).

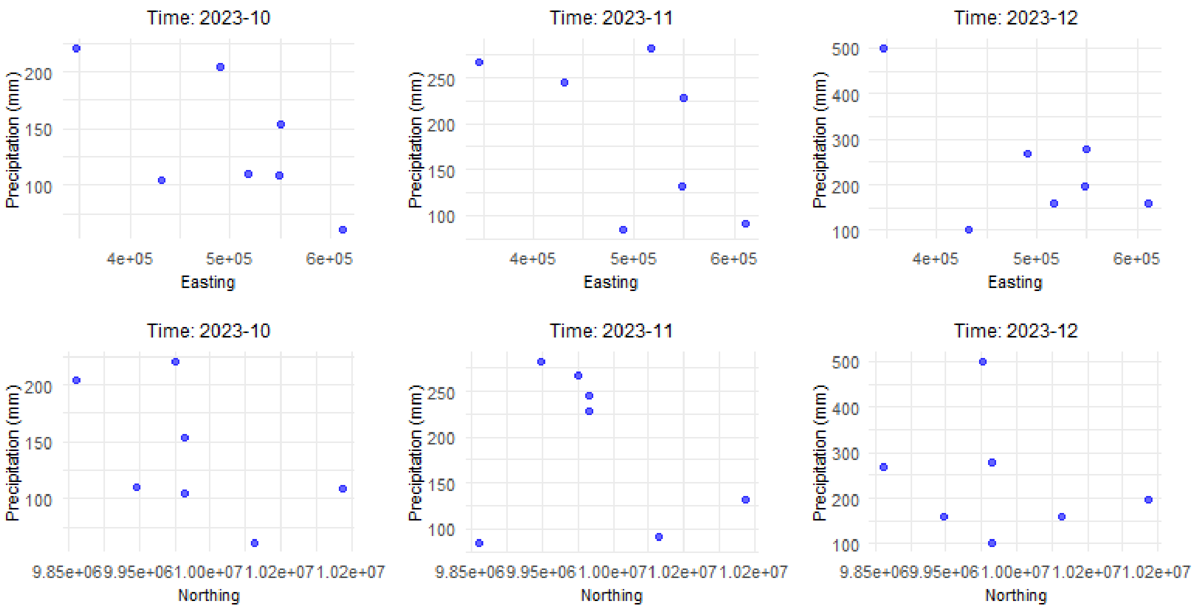

Figure 1. Precipitation based on longitude (easting) and latitude (northing)

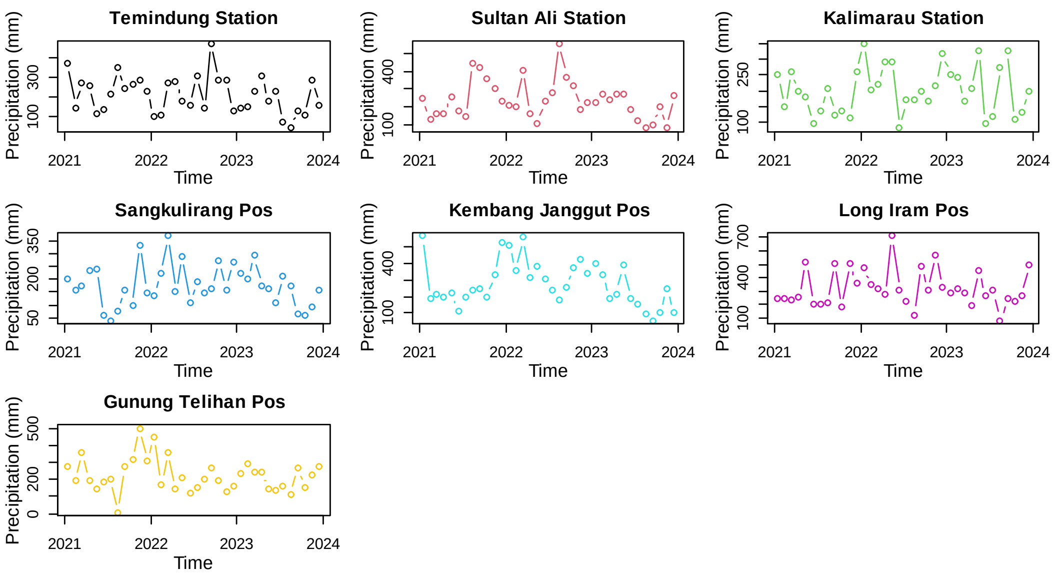

Figure 2. Precipitation for each observation point

2. Spatio-Temporal Kriging

ST-Kriging modeling uses a semivariogram to account for the variability between data points, as well as the relationships between spatial, temporal, and joint spatio-temporal distances. The results of matching various theoretical models to the empirical semivariogram produce the RMSE presented in Table 1. The simple sum-metric model, where the spatial semivariogram follows an exponential model while temporal and joint semivariogram models follow a gaussian model, is identified as the best spatio-temporal semivariogram model, producing the lowest RMSE of 2493.687.

Table 1. RMSE Spatio-Temporal Semivariogram Model

RMSE Spatio-Temporal Model	Joint Model	Spatial and Temporal Semivariogram Model				Joint Model	
		Exp+Exp	Exp+Gau	Gau+Exp	Gau+Gau	Exp	Gau
Metric	·	·	·	·	·	2523.381	2523.475
Sum-metric	Exp	2522.348	2522.350	2522.352	2522.349	·	·
	Gau	2502.212	2501.695	2501.505	2493.735	·	·
Simple sum-metric	Exp	2523.751	2523.756	2523.756	2523.756	·	·
	Gau	2493.839	2493.687	2493.738	2493.721	·	·

*Exp+Gau means spatial semivariogram follows an exponential model and the temporal semivariogram follows a gaussian model

The simple sum-metric model provides the best fit for the spatio-temporal semivariogram, with the spatial component following an exponential model, while the temporal and joint components follow a Gaussian model. This model yields the lowest RMSE of 2493.687, indicating the best performance among the tested models. The fitted semivariogram model is:

$$\gamma(\boldsymbol{h},u) = 7317.03 + \gamma_s(\boldsymbol{h}) + \gamma_t(u) + \gamma\left(\sqrt{\|\boldsymbol{h}\|^2 + (84{,}458.50|u|)^2}\right) \tag{9}$$

with component functions:

$$\gamma_s(|\boldsymbol{h}|) = 1664.27\left\{1 - exp\left(-\frac{|\boldsymbol{h}|}{56{,}414.54}\right)\right\}$$

$$\gamma_t(u) = 15{,}306.94\left\{1 - exp\left(-\frac{|u|^2}{16{,}599.69^2}\right)\right\}$$

$$\gamma\left(\sqrt{\|\boldsymbol{h}\|^2 + (84{,}458.50|u|)^2}\right) = 3857.67\left\{1 - exp\left(-\frac{\|\boldsymbol{h}\|^2 + (84{,}458.50|u|)^2}{18{,}3974.10^2}\right)\right\}$$

Figure 3 presents the spatio-temporal empirical semivariogram, which illustrates the sample variability of precipitation phenomena in East Kalimantan, compared to the simple sum-metric semivariogram, identified as the best-fitting spatio-temporal semivariogram.

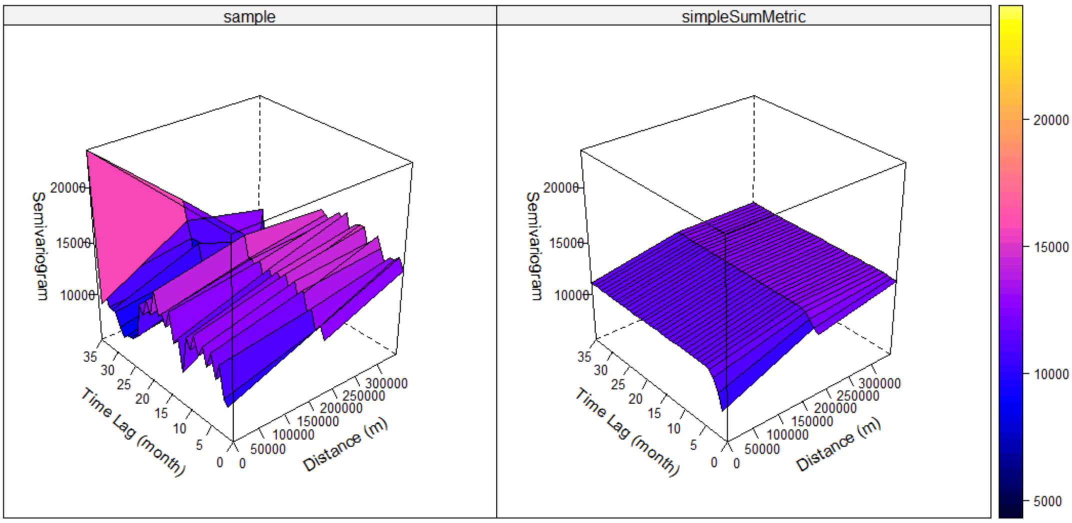

Figure 3. Empirical semivariogram and the best fitting (simple sum-metric) semivariogram

The nugget value of 7317.03 indicates unexplained semivariance at zero distance, likely due to measurement errors. The anisotropy correction of 84,458.50 m suggests that one temporal unit is equivalent to 84.46 km in spatial distance, allowing alignment between spatial and temporal correlation scales.

3. Spatio-Temporal Median Polish

Outlier detection using the Z-Score method identified precipitation in West Kutai during May 2022 as an outlier (Z = 4.247). Given that such extreme values can bias interpolation models assuming normality, median polish kriging was adopted to improve robustness. Median polish decomposes the data into overall mean, spatial effect, time effect, and residuals through iterative median subtraction. The overall mean was 230.775 mm. Spatial effects ranged from -65.525 mm to 69.175 mm, while temporal effects showed considerable month-to-month variation. Residual analysis revealed a remaining outlier (Z = 3.581) in West Kutai during May 2022, indicating that while the influence of outliers was reduced, it was not fully neutralized. This persistence can occur because median polish addresses global trend structures but does not explicitly detect or remove all local anomalies. As a result, residual outliers may still propagate through the kriging stage, subtly affecting the final predictions. Thus, although ST-MPK improves robustness compared to conventional methods, its effectiveness is bounded when faced with extremely skewed observations.

a. Median Polish Spatial Effect Modeling with Kriging

   Spatial effects extracted from median polish showed a clear decreasing trend from west to east. Consequently, universal kriging was used to interpolate these effects. Among tested semivariogram models (spherical, exponential, Gaussian), the exponential model performed best with the smallest SSE (0.000048). The model parameters were:

   1) Nugget: 284.452
   2) Sill: 499
   3) Effective Range: 166,796.6
   4) Range: $\frac{\text{Effective Range}}{3} = 55{,}598.867$

The theoretical semivariogram equation used:

$$\gamma_s(|\boldsymbol{h}|) = 499\left\{1 - exp\left(-\frac{|\boldsymbol{h}|}{55{,}589.867}\right)\right\} \tag{10}$$

(Jannah et al., 2025)

The nugget term suggests short-scale measurement noise or microscale variability. The relatively large range highlights a broad spatial dependency, confirming spatial smoothness in the median-polished effects. This modeling ensures that large-scale geographic patterns are preserved in the interpolated surface.

b. Median Polish Time Effect Modeling with ARIMA

Temporal patterns from the median polish component showed non-seasonal fluctuations. After a second-order differencing process, the data achieved stationarity, and the $ARIMA(1{,}2{,}0)$ model was selected. The AR coefficient was significant ($\phi = -0.881$), and the ARIMA equation is given by Jannah et al. (2025):

$$\tau_t = 2\tau_{t-1} - \tau_{t-2} - 0.881(\tau_{t-1} - 2\tau_{t-2} + \tau_{t-3}) + a_t \tag{11}$$

The AR parameter was statistically significant, and diagnostic checks confirmed model adequacy. The ARIMA model achieved a MAPE of 21.589%, indicating strong temporal prediction ability.

c. Spatio Temporal Kriging Modeling on Median Polish Model Residuals

Residuals were interpolated using ST-Kriging with a simple sum-metric semivariogram model. The best-fit configuration adopted gaussian models for spatial, temporal, and joint components, minimizing RMSE to 2668.869. The model was defined as:

$$\gamma(\boldsymbol{h}, u) = 6993.967 + \gamma_s(\boldsymbol{h}) + \gamma_t(u) + \gamma_{st}\left(\sqrt{\|\boldsymbol{h}\|^2 + (3229.449|u|)^2}\right) \tag{12}$$

with,

$$\gamma_s(|\boldsymbol{h}|) = 760{,}222.3\left\{1 - exp\left(-\frac{|\boldsymbol{h}|^2}{2{,}771{,}718.9^2}\right)\right\}$$

$$\gamma_t(u) = 0\left\{1 - exp\left(-\frac{|u|^2}{651{,}794.97^2}\right)\right\}$$

$$\gamma_{st}\left(\sqrt{\|\boldsymbol{h}\|^2 + (3229.449|u|)^2}\right) = 0\left\{1 - exp\left(-\frac{\|\boldsymbol{h}\|^2 + (3229.449|u|)^2}{55{,}718.34^2}\right)\right\}$$

(Jannah et al., 2025)

The nugget of 6993.967 reflects unexplained variance, while the anisotropy correction of 3229.449 m implies that one temporal unit corresponds to 3.229 km, capturing finer spatio-temporal dependencies.

d. Spatio Temporal Median Polish Kriging

The spatio-temporal median polish kriging model, enhanced with ARIMA, integrates four components: the overall mean (230.775 mm), kriged spatial effects based on equation (10), ARIMA-modeled temporal effects in equation (11), and residual interpolation via ST-Kriging using the semivariogram in equation (12). The complete model is summarized in equation (13),

$$\hat{Z}(\boldsymbol{s_0}, t_0) = 230.775 + \sum_{i=1}^{7} \lambda_i \alpha(\boldsymbol{s}_i) + 2\tau_{t-1} - \tau_{t-2} - 0.881(\tau_{t-1} - 2\tau_{t-2} + \tau_{t-3}) + a_t + \sum_{l=1}^{252} \lambda_l e(s_l, t_l) \tag{13}$$

4. Model Performance

The ST Kriging model achieved an RMSE of 84.05, MAE of 69.95, and MAPE of 52.67%, indicating reasonable absolute accuracy but limited relative accuracy. Conversely, the ST-MPK model produced higher RMSE (122.44) and MAE (91.35), yet achieved a lower MAPE of 44.83%, suggesting superior proportional prediction performance. This distinction is critical for real-world applications: while RMSE and MAE indicate precision in absolute terms, MAPE better reflects the model's adaptability to local extremes. In the context of water resource management and flood risk mitigation, accurate relative predictions are essential. A lower MAPE means ST-MPK more effectively captures both very high and very low precipitation values, key for identifying early signs of flood or drought. This robustness to outliers and extreme events makes ST-MPK more suitable for operational decision-making in dynamic and environmentally vulnerable regions such as East Kalimantan.

D. CONCLUSION AND SUGGESTIONS

This study successfully compared two precipitation models: spatio-temporal kriging (ST-Kriging) and spatio-temporal median polish kriging (ST-MPK). Using consistent datasets and performance metrics (RMSE, MAE, and MAPE), the comparison revealed key differences in predictive capabilities. The results demonstrate that although the ST-MPK model yielded slightly higher RMSE and MAE values compared to ST-Kriging, it achieved a notably lower MAPE, suggests that ST-MPK provides more accurate relative predictions, particularly in regions with highly variable or extreme precipitation values. The robustness of ST-MPK is attributable to its use of the median polish procedure, which decomposes the data into additive components and reduces the influence of outliers by focusing on medians rather than means. This makes it more resilient in the presence of anomalous events such as localized heavy precipitation, which are common in tropical climates like East Kalimantan. This robustness is especially important in the context of hydrological modeling and disaster management. Outliers, if not properly handled, can distort spatial interpolation and lead to unreliable forecasts, particularly in flood-prone areas. By mitigating their impact, ST-MPK ensures more stable and realistic precipitation estimates, which are crucial for accurate flood risk assessment and sustainable water resource planning.

Moreover, to enhance the spatial resolution and predictive strength of the model, future study should incorporate a denser network of observation stations. A greater number of data points would better capture local precipitation variability, reduce interpolation uncertainty, and improve the reliability of semivariogram estimation, especially for short-range spatial correlations. This would allow both spatial and spatio-temporal models to more precisely reflect true precipitation dynamics across East Kalimantan's diverse topography and microclimates.

REFERENCES

Abdullah, A. S., Matoha, S., Lubis, D. A., Falah, A. N., Jaya, I. G. N. M., Hermawan, E., & Ruchjana, B. N. (2018). Implementation of Generalized Space Time Autoregressive (GSTAR)-Kriging model for predicting rainfall data at unobserved locations in West Java. *Applied Mathematics and Information Sciences*, *12*(3), 607–615. https://doi.org/10.18576/amis/120316

Adiguna, I. B. A. P., Nuarsa, I. W., & Puspitha, N. L. P. R. (2021). Pengaruh Suhu Permukaan Laut terhadap Curah Hujan di Pulau Bali Tahun 2009-2018. *Journal of Marine and Aquatic Sciences*, *7*(2), 214. https://doi.org/10.24843/jmas.2021.v07.i02.p10

Chen, Y., Paschalis, A., Wang, L. P., & Onof, C. (2021). Can we estimate flood frequency with point-process spatial-temporal rainfall models? *Journal of Hydrology*, *600*. https://doi.org/10.1016/j.jhydrol.2021.126667

De Carvalho, J. R. P., Nakai, A. M., & Monteiro, J. E. B. A. (2016). Modelagem espaço temporal para imputação de dados para séries de precipitação diária em zonas homogêneas. *Revista Brasileira de Meteorologia*, *31*(2), 196–201. https://doi.org/10.1590/0102-778631220150025

Islam, N., Kashem, A., Das, P., Ali, M. N., & Paul, S. (2024). Prediction of high-performance concrete compressive strength using deep learning techniques. *Asian Journal of Civil Engineering*, *25*(1), 327–341. https://doi.org/10.1007/s42107-023-00778-z

Jannah, F. M., Fitriani, R., & Pramoedyo, H. (2025). Spatio-Temporal Median Polish Kriging with ARIMA Integration for Monthly Precipitation Interpolation in East Kalimantan. *JTAM Journal*, *9*(2), 568–586. https://doi.org/https://doi.org/10.31764/jtam.v9i2.29570

Katipoğlu, O. M. (2022). Spatial analysis of seasonal precipitation using various interpolation methods in the Euphrates basin, Turkey. *Acta Geophysica*, *70*(2), 859–878. https://doi.org/10.1007/s11600-022-00756-0

Liu, P., & Tung, Y. K. (2020). Spatial interpolation of rain-field dynamic time-space evolution based on radar rainfall data. *Hydrology Research*, *51*(3), 521–540. https://doi.org/10.2166/nh.2020.115

Martínez, W. A., Melo, C. E., & Melo, O. O. (2017). Median Polish Kriging for space–time analysis of precipitation. *Spatial Statistics*, *19*(1), 1–20. https://doi.org/10.1016/j.spasta.2016.10.003

Montero, J.-M., Fernández-Avilés, G., & Mateu, J. (2015). *Spatial and Spatio-Temporal Geostatistical Modeling and Kriging* (1st ed.). John Wiley & Sons, Ltd. https://doi.org/10.1002/9781118762387

Murthy, V., & Okunade, A. (2018). Is the health care price inflation in US urban areas stationary?: Evidence from panel unit root tests. *Journal of Economics, Finance and Administrative Science*, *23*(44), 77–94. https://doi.org/10.1108/JEFAS-02-2017-0043

Olanrewaju, R., Ekiotuasinghan, B., & Akpan, G. (2017). Analysis of rain fall pattern and flood incidences in Warri metropolis, Nigeria. *Geography, Environment, Sustainability*, *10*(4), 83–97. https://doi.org/10.24057/2071-9388-2017-10-4-83-97

O'Leary, B., Reiners, J. J., Xu, X., & Lemke, L. D. (2016). Identification and influence of spatio-temporal outliers in urban air quality measurements. *Science of The Total Environment*, *573*(1), 55–65. https://doi.org/10.1016/j.scitotenv.2016.08.031

Pertiwi, M. A., Kahar, S., Sasmito, B., & Marpaung, S. (2015). Analisis Korelasi Suhu Permukaan Laut Terhadap Curah Hujan dengan Metode Penginderaan Jauh Tahun 2012-2013 (Studi Kasus : Kota Semarang). *Jurnal Geodesi Undip Januari*, *4*(1), 61–71. https://doi.org/https://doi.org/10.14710/jgundip.2015.7639

Raja, N. B., Aydin, O., Türkoğlu, N., & Çiçek, I. (2017). Space-time kriging of precipitation variability in Turkey for the period 1976–2010. *Theoretical and Applied Climatology*, *129*(1–2), 293–304. https://doi.org/10.1007/s00704-016-1788-8

Rohma, N. N., Pramoedyo, H., & Astutik, S. (2023). Perbandingan Pendugaan Metode Ordinary Kriging dan Metode Ordinary Kriging dengan Teknik Jackknife. *MAp (Mathematics and Applications) Journal*, *2*(4), 101–111. https://doi.org/https://doi.org/10.15548/map.v4i2.4736

Ruslana, Z. N., Prihatin, R. S., Sulistiyowati, S., & Nugroho, K. (2024). Application of the Arima Method to Prediction Maximum Rainfall at Central Java Climatological Station. *Sinkron*, *8*(4), 2135–2141. https://doi.org/10.33395/sinkron.v8i4.13984

Sari, F. P., & Atsidiqi, S. N. (2020). Investigasi Pengaruh Skenario Modifikasi Urbanisasi pada Perubahan Hujan di Kota Makassar. *Prosiding SNFA (Seminar Nasional Fisika Dan Aplikasinya)*, *5*(1), 85–96. https://doi.org/10.20961/prosidingsnfa.v5i0.46597

Shand, L., & Li, B. (2017). Modeling nonstationarity in space and time. *Biometrics*, *73*(3), 759–768. https://doi.org/10.1111/biom.12656

Sudinda, T. W. (2020). Pemanfaatan Air Hujan untuk Memenuhi Kebutuhan Air Baku Jangka Panjang Ibu Kota Negara. *Construction Engineering and Sustainable Development*, *3*(1), 1–48. https://www.e-journal.trisakti.ac.id/index.php/sipil/article/view/13654

Sun, Y., & Genton, M. G. (2012). Functional Median Polish. *Journal of Agricultural, Biological, and Environmental Statistics*, *17*(3), 354–376. https://doi.org/10.1007/s13253-012-0096-8

Tutmez, B. (2014). Analyzing non-stationarity in cement stone pit by median polish interpolation: a case study. *Journal of Applied Statistics*, *41*(2), 454–466. https://doi.org/10.1080/02664763.2013.840274

Varouchakis, E. A., Hristopulos, D. T., Karatzas, G. P., Perez, G. A. C., & Diaz, V. (2021). Spatiotemporal geostatistical analysis of precipitation combining ground and satellite observations. *Hydrology Research*, *52*(3), 804–820. https://doi.org/10.2166/nh.2021.160

Verdin, A., Funk, C., Rajagopalan, B., & Kleiber, W. (2016). Kriging and local polynomial methods for blending satellite-derived and gauge precipitation estimates to support hydrologic early warning systems. *IEEE Transactions on Geoscience and Remote Sensing*, *54*(5), 2552–2562. https://doi.org/10.1109/TGRS.2015.2502956

Yang, X., Yang, Y., Li, K., & Wu, R. (2020). Estimation and characterization of annual precipitation based on spatiotemporal kriging in the Huanghuaihai basin of China during 1956–2016. *Stochastic Environmental Research and Risk Assessment*, *34*(9), 1407–1420. https://doi.org/10.1007/s00477-019-01757-0

Zhang, W., Liu, D., Zheng, S., Liu, S., Loáiciga, H. A., & Li, W. (2020). Regional precipitation model based on geographically and temporally weighted regression kriging. *Remote Sensing*, *12*(16), 1–19. https://doi.org/10.3390/RS12162547